Proteasome−Cytochrome *c* Interactions: A Model System for Investigation of Proteasome Host−Guest Interactions†

Holly A. Huffman,‡,§ Mehrnoosh Sadeghi,‡,⊥ Erika Seemuller,|| Wolfgang Baumeister,|| and Michael F. Dunn*,‡

Department of Biochemistry, University of California, Riverside, California 92521, and Department of Structural Biology, Max-Plank-Institut für Biochemie, D-821521 Martinsried, Muchen, Germany

Received December 5, 2002; Revised Manuscript Received April 3, 2003

ABSTRACT: Owing to its high thermal stability and structural simplicity, the archaebacterium *Thermoplasma Acidophilum* 20S proteasome was selected for mechanistic studies in this work. This oligomeric enzyme complex consists of a barrel-shaped 20S core (∼700kDa) comprised of four stacked seven-membered rings with a $\alpha_7\beta_7\beta_7\alpha_7$ subunit structure situated around a 7-fold symmetry axis. The hollow interior of the proteasome has three large interconnected chambers with narrow (13 Å diameter) entrances from solution located at either end of the barrel. The 14 β-subunit proteolytic sites are located on the inner surface of the central chamber. Herein, we demonstrate that unfolded horse heart ferricytochrome *c* (Cyt *c*) is a novel chromophoric probe for investigation of the mechanism of proteasome action. Under conditions of temperature and denaturant which unfold Cyt *c* but do not alter the thermophilic proteasome, Cyt *c* is extensively cleaved by the proteasome. Ten peptides were isolated and sequenced from the proteasome digest. Analysis of the cleavage products established that unfolded Cyt *c* and its covalently attached heme prosthetic group are translocated to the central chamber where proteolysis occurs. In the presence of site-specific inhibitors of the proteasome, we demonstrate that unfolded cytochrome *c* can be sequestered inside the proteasome complex. Upon cooling, a quasistable host−guest complex is formed. Analysis of the complex via UV/visible spectroscopy and mass spectrometry gave evidence that the sequestered Cyt *c* is essentially intact within the inhibited proteasome. High-performance liquid chromatography data show that (1) complexes with an apparent stoichiometry of approximately one Cyt *c* per proteasome can be formed and (2) when inhibition is removed from the complex, a rapid turnover of the sequestered Cyt *c* occurs.

The biological function of the proteasome is to carry out the controlled degradation of proteins within the cell (*1*−*3*). The proteasome found in archaebacteria has a simple subunit structure (*3*, *4*). The most well characterized of these is the *Thermoplasma acidophilum* complex, which consists of a 20S core (∼700 kDa) comprised of four stacked seven-membered rings with an $\alpha_7\beta_7\beta_7\alpha_7$[1] subunit arrangement, comprised of identical α-subunits and identical β-subunits (Figure 1A,B). The archaebacteria proteasomes, like their eukaryotic relatives, appear to require a capping protein structure in vivo for unfolding and translocation of substrate proteins into the barrel (*3*, *5*, *6*). These proteasomes also may be involved in the removal of regulatory proteins of programmed transitory existence. The critical role played by the *T. acidophilum* proteasome in cell response to stress (*7*), coupled with its simple structure and thermal stability, make this complex an important subject for proteasome structure−function studies (*3*, *8*−*16*). Both the eukaryotic and prokaryotic proteasomes cleave protein substrates into peptide fragments including peptides of ∼7−9 amino acid residues (7-mers, 8-mers, and 9-mers). In eukaryotes, these peptides function in the immune response system as the recognition peptides for the major histocompatibility complex (*1*−*3*, *5*). The role played by the peptides formed in prokaryotic systems is not understood (*14*).

Two breakthroughs concerning the *T. acidophilum* proteasome make it attractive for mechanistic studies. The *T. acidophilum* proteasome has been cloned and overexpressed in *E. coli* (*15*), making the complex available for biophysical structure−function studies. The structure of the proteasome was solved at 3.4 Å resolution (*11*) (Figure 1A,B). This structure shows the $\alpha_7\beta_7\beta_7\alpha_7$ complex consists of a hollow barrel with D_7 symmetry comprised of two α- and two β-rings of seven subunits each, with the two β-rings flanked by the two α-rings (Figure 1A,B). The barrel is 150 Å long with a 110 Å diameter. The hollow interior has three large interconnected chambers with narrow (13 Å diameter) entrances from solution at either end of the barrel. Wenzel and Baumeister (*10*) established that entry of unfolded

† Supported by a grant from the Academic Senate of the University of California at Riverside.

* Corresponding author. Phone: 909-787-4235. Fax: 909-787-4434. E-mail: michael.dunn@ucr.edu.

‡ University of California, Riverside.

§ Present address: Department of Chemistry and Biochemistry, Arizona State University, Tempe, AZ 85287.

|| Max-Plank-Institut für Biochemie.

⊥ Present address: Invitrogen Corporation, Carlsbad, CA 92008

[1] Abbreviations: $\alpha_7\beta_7\beta_7\alpha_7$, the proteasome from *T. acidophilum*; Ala-Ala-Phe-AMC, L-Ala-L-Ala-L-Phe-7-amido-4-methylcoumarin; Cyt *c*, horse heart ferricytochrome *c*; RP-HPLC, reversed-phase high-performance liquid chromatography; SEC-HPLC, size exclusion high-performance liquid chromatography; MALDI, matrix-assisted laser desorption ionization; PSD, post source decay.

10.1021/bi027310+ CCC: $25.00
Published on Web 07/01/2003

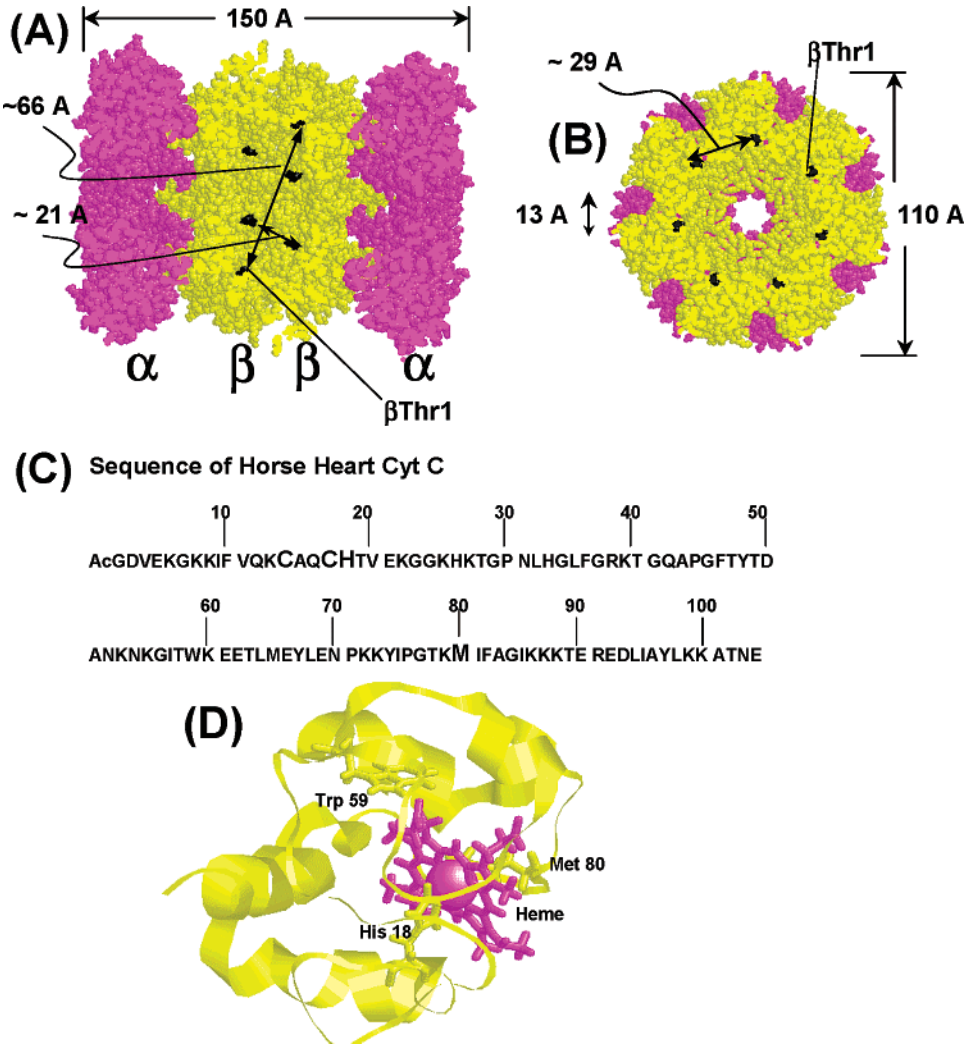

FIGURE 1: The structures of the *T. acidophilum* proteasome and horse heart ferricytochrome *c* (Cyt *c*). Side (A) and top (B) views of space filling models with 50% of the protein cut away to show the inner cavities. The longest distance between β-sites (~66 Å) is shown, along with dimensions for the opening into the barrel (~13 Å), the shortest distance between sites in a β-ring (~29 Å), the shortest distance between the sites of two rings (~21 Å), and the overall dimensions. Colors: α-subunits (magenta = dark gray), β-subunits (yellow = light gray), β-Thr1 (black). (Coordinates taken from Protein Database entry 1PMA). Sequence (C) and structure (D) of horse heart ferricytochrome *c*. The structure shows the protein as a ribbon and the heme as a stick model. Trp 59 and the axial ligands, His 18 and Met 80, are also shown as sticks. The heme is covalently attached at Cys 14 and Cys 17. (Coordinates from Protein Database entry 1HRC)

polypeptides into the proteasome barrel is via these ports (Figure 1A,B). The central chamber (~ 66 × ~66 × ~40 Å) has a volume of ~ 84 nm^3, while the two anterior chambers (~50 × ~50 × ~40 Å) have volumes of ~ 59 nm^3 (*16*). The 14 protease active sites (one per β-subunit) are located on the interior surface of the central chamber (*11*). Structural and site-directed mutation work (*11*, *15*−*17*) has shown that the sites have an unusual catalytic triad, Glu-CO_2^-, Thr-α-NH_2, and Thr-OH, where the Thr-OH is the nucleophile. Thus, the proteasome is a member of the Ntn (N-terminal nucleophile) family of proteases (*16*).

Owing to the thermophilic nature of its parent organism, the *T. acidophilum* proteasome exhibits high thermal stability and a temperature optimum of 85−90 °C for peptide hydrolysis (*12*, *18*). The pH optimum for catalytic activity is pH ~8.5 (*18*). The work of Dahlmann et al. (*18*) and Akopian et al. (*12*) have shown the proteasome is mildly activated by a variety of reagents, including urea and guanidine hydrochloride (GuHCl). Strong, specific inhibitors of the proteasome include Calpain-1 (*11*, *20*), clasto-lactacystin-β-lactone (*11*, *19*−*21*), synthetic peptide aldehydes (*21*, *22*), peptide vinyl sulfones (*23*), and 3,4-dichloroisocoumarin (*19*). These all covalently react with the β-active site Thr-1 hydroxyl.

Normal cell function and survival is dependent on protein degradation; control of this degradation is essential to prevent the destruction of proteins not targeted for destruction. Confinement of degradation to a nanocompartment is a key cellular strategy in archaea, bacteria, and eukarya. It is now apparent that the microenvironments provided within the GroEL/GroES chaperonin system of nanocompartments is tailored to modulate their interactions with unfolded and folded forms of the polypeptide substrate (*24*, *25*−*28*). It is likely that the proteasome nanocompartments are designed both to stabilize the unfolded substrate and to facilitate translocation of the substrate protein from solution into the central chamber. However, the detailed roles played by the anterior and central chambers in the translocation mechanism are unknown.

Protein folding and unfolding are mechanistically related transformations in the cell that occur within self-compartmentalizing protein structures. Several examples of host−

guest complexes with molecular chaperonins have been studied as folding intermediates and folding product complexes (see refs *25*−*28*); however, no such complexes have been reported for the proteasome. The proteasomes and the ClpP systems evolved as protein "death machines" (*36*, *37*), while the chaperonins evolved as "life support machines" for nascent proteins. This work investigates the use of heat and denaturants as a device for introducing unfolded protein substrates into the proteasome and presents a preliminary physical characterization of host−guest complexes formed between horse heart Ferricytochrome *c* (Cyt *c*) (Figure 1C,D) and proteasome that has been inactivated by reaction with site-specific small molecule inhibitors. Cyt *c* (Figure 1A,B) was chosen as a substrate for the *T. acidophilum* proteasome in these studies for several reasons, including (a) its small size (12 364 Da), (b) the wealth of folding information (*40*−*50*), (c) the extensive Cyt *c* structural database (*51*−*54*), (d) the useful spectroscopic signatures of Cyt *c* folding arising from the heme chromophore (covalently linked via Cys 17 and Cys 19), and (e) the extensive use of Cyt *c* as a mass spectrometer protein standard. This work is intended to set the stage for the investigation of the molecular mechanism of action concerning protein−protein interactions between the proteasome and protein substrates.

EXPERIMENTAL METHODS

Substrates, Inhibitors, and General Chemicals. Peptide substrate analogues and horse heart ferricytochrome *c* (Cyt *c*) were purchased from Sigma. Proteasome inhibitor Calpain-1 was purchased from Sigma, and clasto-lactacystin-β-lactone was purchased from CalBiochem. Ni−NTA agarose gel was purchased from Qiagen. Other chemicals were purchased from Sigma and were of the highest purity available.

Isolation and Characterization of the T. acidophilum Proteasome. The $\alpha_7\beta_7\beta_7\alpha_7$ *T. acidophilum* proteasome was prepared via published procedures (*38*). The β-subunit is elongated at the C-terminal end with an affinity tag consisting of six consecutive His residues (*38*). Purification was carried out using an Ni−NTA agarose gel affinity column for His-tagged proteins. Cryo-electron micrographs (cryo-EM) of these proteasome preparations showed the characteristic barrel-like structure of the assembled proteasome, and these preparations exhibited proteolytic activities for the cleavage of the chromogenic/fluorogenic substrate, Ala-Ala-Phe-AMC, comparable to those reported in the literature (*12*, *18*).

Optical Spectroscopy. A Hewlett-Packard 8452A diode array UV/visible spectrophotometer interfaced with a microcomputer was used to collect reaction information in both the spectrophotometer's kinetic and static modes. Protein concentrations were determined via UV/vis spectroscopy by application of the Beer−Lambert law using $\epsilon_{280} = 3.6 \times 10^5\ M^{-1}\ cm^{-1}$, a value verified using the bicinchoninic acid method (*39*). A SPEX 1680 spectrofluorometer interfaced with a SpectrAcq microcomputer was used for Cyt *c* unfolding studies. Studies with Cyt *c* only, were conducted using $\lambda_{ex} = 280$ nm; studies of Cyt *c* in the presence of the proteasome were conducted using $\lambda_{ex} = 295$ nm to minimize interference from proteasome tyrosines. All slit widths employed were 2.5 nm bandwidth. A Jasco J-600 polarimeter was used to collect circular dichroism data for the native and denatured conformational states of Cyt *c*. The instrument parameters were set as follows: bandwidth = 2 nm, sensitivity = 50 mdeg/fs, wavelength range = 250−450 nm, step resolution = 1 nm, scan speed = 20 nm/min, and time constant = 1 s.

High-Performance Liquid Chromatography. Analysis of the fragments generated from proteasome digested Cyt *c* was performed using a Waters LC625 HPLC system equipped with a model 996-photodiode array (PDA) detector. Samples of 500 μL were loaded onto a Waters delta pack C18 narrow bore column equilibrated in 98% solvent A (0.1% TFA in water) and 2% solvent B (80% acetonitrile, 0.1% TFA in water) at a flow rate of 0.2 mL/min. The peptides were eluted with a three-step linear gradient from 2% to 98% of solvent B consisting of the following steps: 0−60 min, 2−37.5% B; 60−90 min, 37.5−75% B; 90−105 min, 75−98% B. Peptide elution was monitored at 210 and 395 nm (wavelengths corresponding to the peptide and heme chromophores in acid media, respectively).

Isolation of Cyt *c*−proteasome complexes was also carried out on the Waters LC625 HPLC system. Samples of 50 μL were loaded onto an analytical Shodex 830 size exclusion column equilibrated with a 20 mM sodium phosphate and 100 mM sodium chloride buffer (pH 6.9) at a flow rate of 0.6 mL/min. Elution was monitored at 210 and 410 nm (wavelengths corresponding to the peptide and heme chromophores in neutral media, respectively).

Incubation Method for Complex Assays. The assays for complex formation, both in the presence and in the absence of inhibitors, were comprised of 3.2 μM proteasome, 150 μM−1.2 mM cytochrome *c*, and 2 M GuHCl. The assays performed with inhibited proteasome also contained either 420 μM *N*-acetyl-leu-leu-norleucinal (Calpain-1), or 192 μM clasto-lactacystin-β-lactone. The inhibitor was preincubated with the proteasome for 10 m, and then the assay mixtures were placed in a water bath/shaker at 53 °C for the desired incubation time. The mixtures then were rapidly cooled to 15 °C for 5 min to allow refolding of uncleaved Cyt *c*. Samples were immediately applied to the Waters HPLC for size exclusion separation of the complex from free Cyt *c*.

Degradation of E(S) Complex Samples. To observe proteasome degradation of Cyt *c* initiated within the E(S) complex (proteasome entrapped Cyt *c*), samples were prepared and isolated using the incubation method described above for complex formation using Calpain-1 as inhibitor. Following isolation of the complex via SEC-HPLC, GuHCl was added to the sample to give a concentration of 2 M and reheated to 53 °C. The initial time (0 min) was withdrawn immediately after the GuHCl was added, but before the reapplication of heat. Samples of 100 μL then were subsequently withdrawn at the desired time intervals, and reaction was quenched by addition of 400 μL 0.1% TFA. These samples then were frozen at −70 °C until analyzed by RP-HPLC.

Mass Spectrometry. Cyt *c* peptide fragments collected after separation by RP-HPLC were analyzed by MALDI and/or MALDI-PSD mass spectrometry. All mass spectra were acquired on a PerSeptive Biosystems Voyager DE-STR equipped with an N_2 laser (337 nm, 3 ns pulse width, 3 Hz repetition rate). Most of the mass spectra were acquired in the reflectron mode with delayed extraction. Reflectron mode gives better resolution and improves the ability to resolve isotopic patterns and to measure the monoisotopic mass;

Table 1: Peptides Identified by Mass Spectrometry, Proteasome Digest of Cyt *c* (Figure 2)

peptide (Figure 2)[a]	sequence (residue numbering)	parent ion mass	amino acid units
Cyt *c*	AcGDVEKGKKIF[10]VQKCAQCHTV[20]EKGGKHKTGP[30]NLHGLFGRKT[40]-GQAPGFTYTD[50]ANKNKGITWK[60]EETLMEYLEN[70]PKKYIPGTKM[80]-IFAGIKKKTE[90]REDLIAYLKK[100]ATNE	12364 (Figure 4D)	104[c]
a	EREDLIAY (90−97)	1008.5[b]	8[d]
b	EYLENPKKYI (66−75)	1296.7[b]	10[d]
c	LENPKKYIPGTKMI (68−81)	1631.9[b]	14[d]
d	KHKTGPNLHG (25−34)	1088.6[b]	10[d]
e	LENPKKYI (68−75)	1004.6[b]	8[d]
f	GIKKKTEREDLIAYLKKA (84−101)	2104.6[b]	18[d]
1	FVQKCAQCHTVEKGGK (10−25)	2427 ± 2.81	16 + heme[e]
2	QKCAQCHTVE (12−21)	1776 ± 1.95	10 + heme[e]
3	AcGDVEKGKKIFVQKCAQCHTVEKGGKHKTG (1−29)	3800 ± 3.28	29 + heme[e]
4	AcGDVEKGKKIFVQKCAQCHTVEKGG (1−24)	3247±3.0	24 + heme[e]

[a] See designations in Figure 2. [b] Monoisotopic mass values. [c] Determined by MALDI. [d] Determined by MALDI, post source decay. [e] MALDI/GPMAW32 analysis.

however, the reflectron mode is restricted to species <8000 Da. Samples were prepared in a calibration matrix consisting of α-cyano-4-hydroxycinnamic acid and subjected to an accelerating voltage of 20 000 V with a grid voltage of 65% and extraction delay time of 125 ns. Samples containing peptides >8000 Da were analyzed in the linear mode using the matrix sinapinic acid. Both matrixes were prepared in a 1:1 (v/v) acetonitrile and 0.1% TFA solvent. To assign sequence, all searches were carried out using the MS-TAG program from the Protein Prospector suite of search tools developed at UCSF by R. P. Baker and K. R. Clauser (http://prospector. ucsf.edu). No restrictions were placed on the allowed protein molecular mass range; the species were restricted to mammals.

RESULTS

Investigation of Cyt c as Substrate Under Steady-State Conditions. When heated in 2 M GuHCl, Cyt *c* undergoes a reversible unfolding transition in the 40−60 °C range to a nearly random coil state (*48*, *55*). Cooling to 25 °C in 2 M GuHCl refolds Cyt *c* to the native structure in ∼100% yield. This reversible unfolding−refolding can be detected by characteristic changes in the UV/vis absorption and fluorescence spectra (data not shown) (*41*). The Trp 59 fluorescence is nearly completely quenched in the folded state (*34*). The indole ring of Trp 59 interacts directly with the heme (Figure 1C,D), and the strong spectral overlap of its emission spectrum with the heme absorbance spectrum causes quenching via energy transfer to the heme. Loss of these interactions and the large increase in distance between the two chromophores due to unfolding causes a >20-fold enhancement of Trp 59 fluorescence (*34*).

The effects of heat and denaturant on the stability and activity of the proteasome were also examined. It was found that heating the proteasome to 57 °C in 2 M GuHCl had little or no effect on the rate of the proteasome-catalyzed cleavage of the small peptide, Ala-Ala-Phe-AMC. SEC-HPLC studies demonstrated that the size of the proteasome was unaffected by this treatment. The experiments of Akopian et al. (*12*) have shown that the activity of the proteasome is slightly activated by GuHCl in the concentration range 0−3 M, conditions similar to those used in our experiments. Consequently, in agreement with earlier studies, when incubated at 53 °C in 2 M GuHCl, the thermophilic

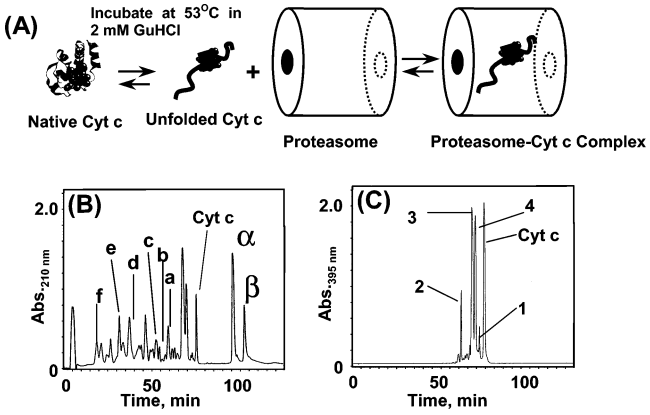

FIGURE 2: (A) Cartoon depicting the preparation of the host−guest complex. RP-HPLC elution profiles at 210 (B) and 395 nm (C) for a 4.5 h proteasome digest of Cyt *c* incubated at 53 °C in 2 M GuHCl at pH 7.5. Peaks a−f in panel B and 1−4 in panel C were sequenced by MALDI-TOF mass spectroscopy and PSD-MALDI (Table 1). Digest conditions: [proteasome] = 3.85 μM; [Cyt *c*] =263 μM. RP-HPLC conditions: samples were dissolved in 0.1% TFA, injected on to the column, and eluted with a 0−80% acetonitrile linear gradient.

T. acidophilum proteasome is stable and catalytically functional (the temperature optimum for proteasome catalysis is ∼85−90 °C) (*12*, *18*).

The proteolytic activity of the proteasome with Cyt *c* as substrate was examined under the reversible unfolding conditions described above (see also Figure 2A), conditions where $\alpha_7\beta_7\beta_7\alpha_7$ is stable but Cyt *c* is substantially unfolded. When there is a 100−500-fold excess of Cyt *c* over proteasome, then under these unfolding conditions degradation of Cyt *c* to peptide fragments is observed within several hours. The reversed phase (RP)-HPLC data measured at 210 nm (Figure 2B) show that prolonged incubation gives a set of peptide fragments with different retention times. Elution profiles measured at 395 nm (the Soret maximum of acid-denatured Cyt *c*) showed that a small subset of these peptides contain covalently bound heme (Figure 2C). Ten peptides (Figure 2B,C, Table 1) were identified via matrix-associated laser desorption ionization (MALDI) and post source decay MALDI (PSD-MALDI) mass spectroscopy. No peptide fragments were detected when Cyt *c* was incubated with the proteasome either at room temperature in 2 M GuHCl or at 53 °C in the absence of GuHCl.

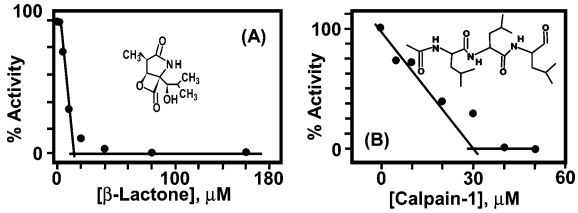

FIGURE 3: (A) Titration of 15 μM proteasome sites with clasto-lactacystin-β-lactone. (B) Titration of 25 μM proteasome sites with Calpain-1.

Inhibition of the Proteasome by Covalent, Site-Specific Modification. The proteasome inhibitor, clasto-lactacystin-β-lactone, is known to acylate the proteasome active site Thr β1 hydroxyl, and due to the extremely slow turnover of this acyl-enzyme, the proteasome is essentially irreversibly inhibited (Figure 3A) (*21*−*23*). As shown in Figure 3A, when the activity of the proteasome, measured as the steady-state rate of cleavage of the small chromophoric/fluorgenic peptide, Ala-Ala-Phe-AMC, is plotted as a function of the concentration of clasto-lactacystin-β-lactone inhibitor, the decrease in rate appears to yield a titration curve with a titration end-point approximately equal to the concentration of proteasome active sites present in solution. This sharp titration end-point indicates that the reaction of the clasto-lactacystin-β-lactone with the proteasome is site-specific and occurs with a [clasto-lactacystin-β-lactone] to [catalytic site] stoichiometry of 1:1.

The proteasome inhibitor, Calpain-1 (*11*, *12*, *15*, *18*, *20*, *22*, *56*, *57*), is a peptide aldehyde that reversibly forms a tetrahedral adduct with the active site Thr hydroxyl (*11*). The titration presented in Figure 3B shows that under the conditions employed in this experiment, Calpain-1 also is a potent inhibitor of the proteasome and provides nearly stoichiometric inhibition of the proteasome.

Isolation of Host−Guest Proteasome−Cyt c Complexes. The demonstration that unfolded Cyt *c* is a competent substrate for the *T. acidophilum* proteasome, together with the small size of native Cyt *c* relative to the central cavity of the proteasome, suggested to us that it would be interesting to attempt trapping unfolded Cyt *c* within the proteasome at 53 °C in 2 M GuHCl and, then, by removal of GuHCl and a shift to room temperature or below, to attempt refolding of the polypeptide inside the proteasome to form a host−guest complex. To prevent scission of unfolded Cyt *c*, the proteasome was preincubated with the reversible inhibitor, Calpain-1, or with the irreversible inhibitor, clasto-lactacystin-β-lactone, prior to addition of denaturant and heat (Figure 3). Two sets of conditions gave proteasome−Cyt *c* complexes, in high yield.

When the clasto-lactacystin-β-lactone-inhibited proteasome is incubated at 53 °C in 2 M GuHCl with a large excess of Cyt *c*, cooling to 15 °C, SEC-HPLC gave a ∼700 kDa heme-containing species coeluting with the proteasome (Figure 4A,B). RP-HPLC of the heme containing proteasome fraction showed components with elution times identical to Cyt *c* (Figure 4C). Only trace amounts of Cyt *c* fragments were detected. MALDI mass spectrometry established that the heme-containing species was intact Cyt *c* (Figure 4D). The yield of complex increased and then saturated as the incubation time increased. Increasing the concentration of Cyt *c* speeded complex formation and increased yield. At

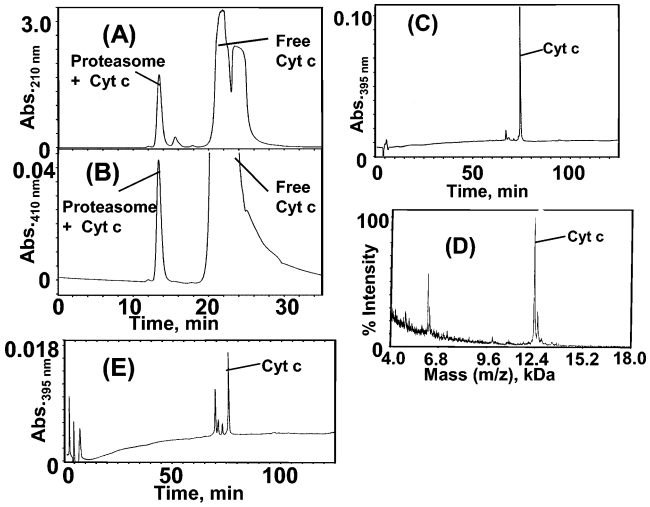

FIGURE 4: (A−D) isolation of the clasto-lactacystin-β-lactone-inhibited proteasome−Cyt *c* host−guest complex. The clasto-lactacystin-β-lactone-inhibited proteasome and Cyt *c* were incubated in 2 M GuHCl at 53 °C and pH 7.5 for 15 min. SEC-HPLC elution profiles at 210 nm (A) and 410 nm (B) show the proteasome fraction exhibits a heme spectrum. When the proteasome fraction in panel B was subjected to RP-HPLC (C), the major heme-containing species has an elution time identical to that of intact Cyt *c*. This species was identified as intact Cyt *c* (mass 12 364 daltons) via MALDI mass spectrometry (D). The stoichiometry of the complex in (B) was ∼1 Cyt *c*/proteasome. (E) The RP-HPLC of host−guest complex from Calpain-1-inhibited proteasome shows cleavage products plus intact Cyt *c*.

long incubation times, some Cyt *c* cleavage occurs. Incubation of Cyt *c* with the clasto-lactacystin-inhibited proteasome at 25 °C in 2 M GuHCl gave only trace amounts of host−guest complex and very little cleavage of Cyt *c*.

When incubation is carried out with a large excess of Cyt *c* in the presence of the reversible inhibitor, Calpain-1 (*11*, *12*), SEC-HPLC (Figure 4) also gave a ∼700 kDa heme-containing fraction coeluting with the proteasome. RP-HPLC of the heme-containing fraction showed the presence of species with elution times identical to intact Cyt *c* (confirmed by MALDI mass spectrometry) and Cyt *c* fragments (Figure 4E). The yield of intact Cyt *c* decreased as the time interval between isolation of the complex by SEC-HPLC and the separation into protein and peptide fragments by RP-HPLC increased, indicating that the SEC-HPLC step separates the reversibly bound Calpain-1, thereby activating the proteasome for cleavage of the entrapped Cyt *c*. Figure 5 shows the SEC-HPLC time course for the accumulation of heme-containing peptides within the Calpain-1-inhibited proteasome. In the presence of Calpain-1, the initially isolated complex consists primarily of intact Cyt *c* (viz. Figure 4E). Again, incubation of Cyt *c* with the Calpain-1-inhibited proteasome at 25 °C gave only trace amounts of host−guest complex and very little cleavage of Cyt *c*.

Spectroscopic Analysis of the Host−Guest Complex. The trapping of host−guest proteasome−Cyt *c* complexes via inhibition of the proteasome with clasto-lactacystin or Calpain-1 (Figure 4) provides the first examples of the preparation of quasi-stable proteasome-substrate complexes for mechanism studies of proteasome catalytic action. Experiments were performed to determine the extent of Cyt *c* refolding that occurs when GuHCl is removed via SEC-HPLC and the host−guest complex is cooling to 15 °C.

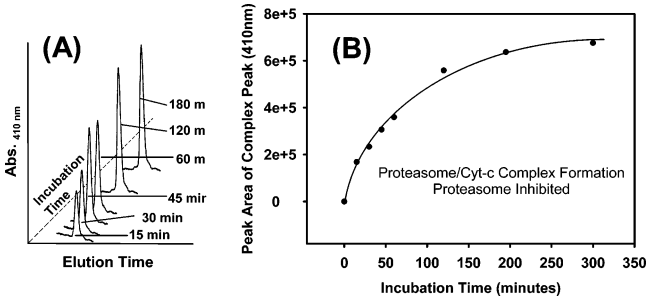

FIGURE 5: Time course for formation of a proteasome−Cyt *c* host−guest complex. (A) SEC-HPLC elution peaks are shown for the heme-containing proteasome complexes formed with 170 mM Cyt *c* and proteasome incubated with 2 M GuHCl at 53 °C in pH 7.5 buffer in the presence of 500 μM Calpain-1. Concentrations: [Cyt *c*] = 170 μM; [Calpain-1] = 500 μM. The dependence of peak area on incubation time is shown in panel B.

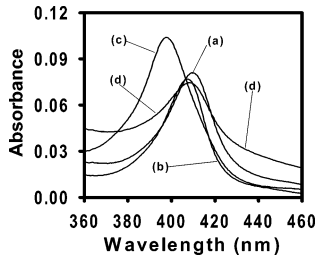

FIGURE 6: Absorption spectra of the Cyt *c* γ-Soret band at (a) pH 7.5 at 25 °C (native, folded state, λ_{max} = 409.5 nm), (b) pH 7.5 in 6 M GuHCl, 25 °C (neutral, unfolded state, λ_{max} = 407.5 nm), (c) pH 2.5 at 25 °C (acid unfolded state, λ_{max} = 395 nm), and (d) the clasto-lactacystin-β-lactone-inhibited proteasome−Cyt *c* host−guest complex at pH 7.5, 25 °C (λ_{max} = 408.5 nm). [Cyt *c*] = (a−c) 1.5 and (d) 0.9 mM.

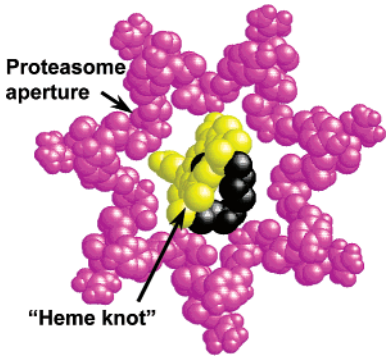

FIGURE 7: Comparison of the van der Waals surfaces of the "heme knot" (Cys 14, Cys 17, and the heme) and of the star-shaped aperture through which polypeptide substrates must pass to gain entry into the proteasome. The proteasome aperture is shown in magenta, the heme in yellow, the heme iron in black, and Cys 14 and Cys 17 in black. (Structures rendered from Protein Database entries 1PMA and 1HRC)

Owing to the small volumes and low concentrations of the complex available for these studies (100−200 μL of ~ 0.9 μM), this work has relied on use of mass spectrometry and UV/vis absorption spectroscopy of the γ-Soret band to partially characterize the physical-chemical state of the sequestered Cyt *c* (Figures 5 and 7).

Examination of the Cyt *c* present in the clasto-lactacystin-β-lactone-inhibited proteasome fraction obtained by RP-HPLC via MALDI mass spectrometry (Figure 4D), establishes that the Cyt *c* that coelutes with the proteasome is not clipped or truncated. The Cyt *c*−proteasome containing fraction gives a UV/vis absorption spectrum (Figure 6d) with a γ Soret band located at λ_{max} = 408.5 nm that is broadened relative to native Cyt *c* free in solution (Figure 6a). This band is located midway between the maxima of the partially unfolded GuHCl-denatured species (407.5 nm, Figure 6b) and the native species (409.5 nm, Figure 6a) (*40*−*43*, *47*, *50*, *55*). Analysis of the γ-Soret band via curve fitting with log-normal curves and correction for light scattering by the proteasome indicates that the blue-shifting of the λ_{max} relative to that of native, free Cyt *c* is not an artifact. Owing to limitations on the concentrations and amounts of host−guest complexes isolated via analytical SEC-HPLC and the small extinction coefficients of the longer wavelength heme bands, we were not able to carefully examine the longer wavelength Cyt *c* spectral signatures.

DISCUSSION

The results of these studies are summarized by the following observations: (a) Cyt *c* is a useful probe for investigation of the physical, chemical, and catalytic properties of the *T. acidophilum* proteasome and its mechanism of action. (b) Proteasome digestion of Cyt *c* at elevated temperatures and in the presence of denaturant (e.g., 53−57 °C and 2 M GuHCl) generates both non-heme and heme-containing peptides. This finding establishes that the combination of heat (53−57 °C) and 2 M GuHCl unfolds Cyt *c* and renders it available to the proteasome for digestion and that the unfolded Cyt *c* finds its way into the central, proteolytic chamber of the proteasome through passive interactions with the proteasome anterior chambers. Thus, the proteasome chambers likely provide an environment that facilitates translocation of the unfolded protein into the central cavity and destabilizes folded Cyt *c*. The anterior chambers of the proteasome appear to possess qualities that favor passage of unraveled protein into the central chamber. The anterior chambers are less hydrophobic than the central chamber (*11*, *16*), and multiple hydrophobic pathways connect α-ring channels with the inner apertures at the entrances to the central chamber. It seems likely that the unfolded polypeptide is directed into the proteolytic core (*16*) via a hydrophobic gradient created by the hydrophobic paths that link the anterior chambers to the central chamber. (c) Incubation of unfolded Cyt *c* with inhibited proteasome (inhibited with either a reversibly bound inhibitor, or an irreversibly bound small inhibitor) allows the isolation and purification of host−guest complexes containing intact Cyt *c*. (d) Cooling to room temperature or below gives proteasome−Cyt *c* complex exhibiting a γ-Soret band that is broadened and shifted with respect to the spectrum of native Cyt *c* free in solution. (e) In the Calpain-1 system, removal of the reversibly bound inhibitor by SEC-HPLC reactivates the proteasome.

Evidence Pertaining to the Mechanism of Peptide Processing. With short peptide substrates, the *T. acidophilum* proteasome exhibits a chymotrypsin-like specificity, with a preference for bond scission at residues with a hydrophobic side chain at P1, the scissile residue (*19*, *21*, *23*). For protein substrates, this preference can be overridden by other factors (*5*, *12*, *13*, *24*). The proteasome-catalyzed digestion of an unfolded protein generates a set of peptides with an average size distribution dominated by hexa- to nona-peptides, but with a broad size distribution (*9*, *10*, *12*, *13*, *21*). The distance between proteasome active sites of adjacent β-subunits, ~29

Å (Figure 1A,B), would favor 7-mers and 8-mers and is likely one factor determining peptide length. Because 7-mers and 8-mers are relatively poor proteasome substrates, cleavage to shorter lengths is negligible (*24*). Specificity preferences, relative affinities of short versus long peptides, and on and off rates versus cleavage rates may also be important (*13*). Goldberg and co-workers (*5*, *12*, *24*) have presented evidence that proteasome-catalyzed protein degradation is a processive process wherein a substrate protein is reduced to small peptides preferentially before initiating proteolysis of another protein molecule.

In this study, 10 peptides were isolated and sequenced from the proteasome-mediated degradation of Cyt *c* (Figures 3 and 5, and Table 1). The six non-heme peptides sequenced are derived from the region of the peptide located on the C-terminal side of the heme. These peptides consist of two 8-mers, two 10-mers, a 14-mer, and an 18-mer (Table 1). Two of the four heme-containing peptides sequenced contain a short peptide segment that spans the Cys residues to which the heme is covalently attached. One is a 10-mer (residues 12−21), and one is a 16-mer (residues 10−25). The other two are much larger peptides (24 and 29 residues), and both include the entire N-terminal region and extend beyond the heme on the C-terminal side. While this sampling of the peptide fragments is incomplete, the size distribution and cleavage pattern is not in good agreement with a simple mechanism for degradation of Cyt *c* wherein the lengths of the peptides generated are determined primarily by the distance between proteasome sites, a conclusion in agreement with Kisselev et al. (*13*).

Since the heme is covalently linked to the Cyt *c* polypeptide via thioether linkages to Cys 14 and Cys 17, the heme group creates a "knot" on the polypeptide "string". Therefore, the complex cleavage pattern obtained could arise from the presence of the "heme knot", and/or the presence of unusual stretches in the sequence (e.g., there are Pro residues at positions 30, 44, 71, and 76).

Inspection of the proteasome X-ray structure shows that the entrances to the proteasome involve α-ring outer apertures of ∼13 Å diameter located on the 7-fold symmetry axis at either end of the barrel-shaped structure (Figures 1A,B, 3, and 10).[2] This aperture is slightly smaller than the dimensions of the heme group with the covalently attached peptide segment, Cys 14-Cys 17 (Figure 7). We considered that the "heme knot" might, via steric clashing with the outer α-ring aperture, restrict the entry of unfolded Cyt *c* into the proteasome. However, as shown in Table 1, the presence of the "heme knot" does not prevent cleavage of the polypeptide at amide linkages close to the heme. This finding argues against a mechanism for cleavage that involves formation of a proteasome−Cyt *c* complex wherein the unfolded Cyt *c* is restricted from full entry into the proteasome interior by van der Waals clashes between the opening into the proteasome and the "heme knot". If steric interactions at the α-ring outer aperture were to prevent passage of the heme into the proteasome interior, then cleavages in the vicinity of the heme could not occur. The distance between this aperture and the nearest active site within the central chamber is at least ∼ 55 Å. Therefore, assuming a fully extended polypeptide, only those peptide bonds of Cyt *c* on either side of the heme at, or more distant than, 55 Å would extend sufficiently into the central cavity to bind to an active site and undergo cleavage. On the N-terminal side of the heme, the peptide would extent sufficiently for cleavage to occur only at residues 1−3, or 1−4 at best. On the C-terminal side of the heme, cleavage would be limited to residues 32−103. In contrast to these predictions, the data in Table 1 show that cleavages are observed at residues significantly closer to the heme. Cleavages actually occur at peptide linkages between amino acid residues 9−10, 11−12, 21−22, 24−25, 25−26, and 29−30. This pattern of cleavages strongly implies that the entire Cyt *c* molecule finds its way into the central chamber of the proteasome. These findings indicate that the loop structures that form the boundary to the α-ring outer aperture (Figure 7) are flexible enough to accommodate passage of the "heme knot".

Akopian et al. (*12*) and McCormack et al. (*21*) found that in short peptides, there is a preference for cleavage at linkages where P1 is hydrophobic, while acidic or basic residues at P1 are generally poor substrates. When the amino acid side chain in position P4 is hydrophobic, binding to the catalytic site is stimulated (*12*), and presumably catalysis of a peptide substrate also would be favored. However, no such pattern is evident in the peptides shown in Table 1. The peptides listed in Table 1 almost all result from cleavages at P1 sites that are hydrophobic (three Tyr, four Ile, two Ala, one Met, one Val). Only two are charged (Lys, Glu), one is neutral polar (Thr), and four are Gly. The somewhat atypical Cyt *c* sequence may be an important factor in determining peptide length. The Cyt *c* polypeptide on the C-terminal side of the heme is quite basic (15 Lys, three His, two Arg, vs only 8 Glu and 2 Asp), and has unusual features consisting of two or more adjacent Lys, one pair at 72 and 73 preceded by Pro, then a stretch of three Lys at 86 to 88, and finally a pair at 99 and 100.

Where is Cyt c Bound? Are Structural Changes induced in the Proteasome? At present, we do not understand the structural origins of the shifted γ Soret band of the clasto-lactacystin-β-lactone-inhibited proteasome−Cyt *c* complex isolated via SEC-HPLC (Figure 6). In solution, the refolding of Cyt *c* from mildly denaturing conditions is not a simple two-state process. A compact form with the Fe^{3+} coordination to Met 80 replaced by His 26, His 33, or H_2O is attained within the first 0.1 ms of the refolding pathway (*58*). These misfolded forms must convert to a Met 80-coordinated form before proceeding to the native conformation. Non-native cis forms of Pro residues also give misfolded states that must isomerize before the native fold can be formed (*44*−*50*). One or more of these misfolded states could account for the perturbed spectrum of the host−guest complex.

When unfolded at neutral pH and 25 °C in GuHCl or urea, the axial position occupied by Met 80 is substituted either with a water molecule or with another protein ligand (His 26 or His 33), and the γ-Soret is blue-shifted, but the heme Fe^{3+} remains low-spin. When unfolded at low pH, the γ-Soret band shifts to 395 nm, and the heme Fe^{3+} becomes high spin. Blue shifting of the Cyt *c* γ Soret band can be a signature of incomplete or incorrect folding with altered

[2] The three internal chambers of the proteasome are separated by two sets of apertures. The α-ring outer apertures with diameter ∼13 Å regulate the passage of molecules from solution into the anterior chambers. The pair of inner apertures situated between the α- and β-rings have diameters of about 18 Å.

coordination at one or both axial positions of the heme. We speculate that within the complex, Cyt *c* either is incompletely folded (an ensemble of folded and unfolded states) or is a folding intermediate (*42*−*45*).

REFERENCES

1. Goldberg, A. L. (1995) *Science 268*, 522−523.
2. Peters, J.-M. (1994) *Trends Biolog. Sci. 19*, 377−382.
3. Baumeister, W., and Lupas, A. (1997) *Curr. Opin. Str. Biol. 7*, 273−278.
4. Tamura, T., Nagy, I., Lupas, A., Lottspeich, F., Cejka, Z., Schoofs, G., Tanaka, K., De Mot, R., S Baumeister, W. (1995) *Curr. Biol. 5*, 766−774.
5. Goldberg, A. L., Akopian, T. N., Kisselev, A. F., Lee, D. H., and Rohrwild, R. (1997) *Biol. Chem. Hoppe-Seyler 378*, 131−140.
6. Zwickl, P., Ng, D., Woo, K. M., Klenk, H.-P., and Goldberg, A. L. (1999) *J. Biol Chem. 274*, 26008−26014.
7. Ruepp, A., Eckerskorn, C., Bogyo, M., and Baumeister, W. (1998) *FEBS Lett. 425*, 87−90.
8. Coux, O., Tanaka, K., Goldberg, A. L. (1996) *Ann Rev. Biochem. 65*, 801−847.
9. Wenzel, T., Eckerskorn, C., Lottspeich, F., and Baumeister, W. (1994) *FEBS Lett. 349*, 205−209.
10. Wenzel, T., and Baumeister, W. (1995) *Nat. Struct. Biol. 2*, 199−204.
11. Lowe, J., Stock, D., Jap, B., Zwickl, P, Baumeister, W., and Huber, R. (1995) *Science 268*, 533−539.
12. Akopian, T. N., Kisselev, A. F., and Goldberg, A. L. (1997) *J. Biol. Chem. 272*, 1791−1798.
13. Kisselev, A., Akopian, T. N., and Goldberg, A. L. (1998) *J. Biol. Chem. 273*, 1982−1989.
14. Baumeister, W., Cejka, Z., Kania, M., and Seemuller, E. (1997) *Biol Chem. 378*, 121−130.
15. Seemuller, E., Lupas, A., Stock, D., Lowe, J., Huber, R., and Baumeister, W. (1995) *Science 268*, 579−583.
16. Baumeister, W., Walz, J., Zuhl, F., and Seemuller, E. (1998) *Cell 92*, 367−380.
17. Brannigan, J. A., Dodson, G. Duggleby, H. J., Moody, P. C. E., Smith, J. L., Tomchick, D. R., Murzin, A. G. (1995) *Nature 378*, 416−419.
18. Dahlmann, B., Kuehn, L., Grziwa, A., Zwickl, P., and Baumeister, W. (1992) *Eur. J. Biochem. 208*, 789−797.
19. Fenteany, G., Standaert, R. F., Lane, W. S., Choi, S., Corey, E. J., and Schreiber, S. L. (1995) *Science 268*, 726−731.
20. Dick, L., R., Cruikshank, A. A., Destree, A. T., Grenier, L., McCormack, T. A., Melandri, F. D., Nunes, S. L., Palombella, V. J., Parent, L. A., Plamonodon, L., and Stein, R. L. (1997) *J. Biol. Chem. 272*, 182−188.
21. McCormack, T. A., Cruikshank, A. A., Grenier, L., Melandri, F. D., Nunes, S. L., Plamondon, L., Stein, R. L., and Dick, L. R. (1998) *Biochemistry 37*, 7792−7800.
22. Mellgren, R. L. (1997) *J. Biol. Chem. 272*, 29899−29903.
23. Bogyo, M., McMaster, J. S., Gaczynska, M., Tortorella, D., Goldberg, A. L., and Ploegh, H. (1997) *Proc. Natl. Acad. Sci. U.S.A. 94*, 6629−6634.
24. Dolenc, I., Seemuller, E., and Baumeister, W. (1998) *FEBS Lett. 434*, 357−361.
25. Ishii, N., Taguchi, H., Sasabe, H., and Yoshida M. (1994) *J. Mol. Biol. 236*, 691−696.
26. Chen, S., Roseman, A. M., Hunter, A. S., Wood, S. P., Burston, S. G., Ranson, N. A., Clarke, A. R., and Saibil, H. R. (1994) *Nature 371*, 261−264.
27. Makino, Y., Amada, K., Taguchi, H., and Yoshida, M. (1997) *J. Biol. Chem. 272*, 12468−12474.
28. Bukau, B., and Horwich, A. L. (1998) *Cell 92*, 351−366.
29. Weber-Ban, E. U., Reid, B. G., Miranker, A. D., and Horwich, A. L. (1999) *Nature 401*, 90−93.
30. Reid, B. G., Fenton, W. A., Horwich, A. L., Weber-Ban, E. U. (2001) *Proc. Natl. Acad. Sci. U.S.A. 98*, 3768−3772.
31. Singh, S. K., Grimaud, R., Hoskins, J. R., Wickner, S., and Maurizi, M. R. (2000) *Proc. Natl. Acad. Sci. U.S.A. 97*, 8898−8903.
32. Kim, Y. I., Burton, R. E., Burton, B. M., Sauer, R. T., Baker, T. A. (2000) *Mol. Cell 5*, 639−648.
33. Ortega, J., Singh, S. K., Ishikawa, T., Maurizi, M. R., and Steven, A. C. (2000) *Mol. Cell 6*, 1515−1521.
34. Hoskins, J. R., Singh, S. K., Maurizi, M. R., and Wickner, S. (2000) *Proc. Natl. Acad. Sci. U.S.A. 97*, 8892−8897.
35. Wah, D. A., Levchenko I., Baker, T. A., and Sauer, R. T. (2002) *Chem. Biol. 11*, 1237−1245.
36. Tanaka, K. (1998) *J. Biochem. 123*, 195−204.
37. Tanaka, K. (1998) *Biochem. Biophys. Res. Comm. 247*, 537−541.
38. Zwickl, P., Lottspeich, F., and Baumeister, W. Expression of functional *T. acidophilum* proteasomes in *E. coli*. (1992) *FEBS 312*, 157−160.
39. Smith, P. K., Krohn, R. I., Hermanson, G. T., Mallia, A. K., Gartner, F. H., Provenzano, M. D., Fujimoto, E. K., Goeke, N. M., Olsen, B. J., Klenk, D. C. (1985) *Anal. Biochem. 150*, 76−85.
40. Babul, J., and Stellwagon, E. (1972) *Biochemistry 11*, 1195−1200.
41. Tsong, T. Y. (1975) *Biochemistry 14*, 1542−1547.
42. Ohgushi, M., and Wada, A. (1983) *FEBS Lett. 164*, 21−24.
43. Goto, Y., Takahashi, N., and Fink, A. L. (1990) *Biochemistry 29*, 3480−3488.
44. Jeng, M.-F., and Englander, S. W. (1991) *J. Mol. Biol. 221*, 1045−1061.
45. Jordan, T., Eads, J. C., and Spiro, T. G. (1995) *Protein Sci. 4*, 716−728.
46. Marmorino, J. L., Lehti, M., and Pielak, G. J. (1998) *J. Mol. Biol. 275*, 379−388.
47. Taler, G., Schejter, A., Navon, G., Vig, I., and Margoliash, E. (1995) *Biochemistry 34*, 14209−14212.
48. Yang, H., and Smith, D. L. (1997) *Biochemistry 36*, 14992−14999.
49. Battistuzzi, G., Borsari, M., Loschi, L., Martinelli, A., and Sola, M. (1999) *Biochemistry 38*, 7900−7907.
50. Indiani, C., de Sanctis, G., Neri, F., Santos, H., Smulevich, G., and Coletta, M. (2000) *Biochemistry 39*, 8234−8242.
51. Takano, T., and Dickerson, R. E. (1981) *J. Mol. Biol. 153*, 95−125.
52. Bushnell, G. W., Louie, G. V., Brayer, G. D. (1990) *J. Mol. Biol. 214*, 585−595.
53. Sanishvili, R., Volz, K. W., Westbrook, E. M., Margoliash, E. (1995) *Structure 3*, 707−716.
54. Banci, L., Bertini, I., Gray, H. B., Luchinat, C., Reddig, T., Rosato, A., Turano, P. (1997) *Biochemistry 36*, 9867−9877.
55. Chen, E., Wood, M. J., Fink, A. L., and Kliger, D. S. (1998) *Biochemistry 37*, 5589−5598.
56. Ditzel, L. Stock D., and Lowe, J. (1997) *J. Biol. Chem 378*, 239−247.
57. Rock, K. L., Gramm, C., Rothstein, L., Clark, K., Stein, R., Dick, L., Hwang, D., and Goldberg, A. L. (1994) *Cell 78*, 761−771.
58. Elove, G. A., Bhuyan, A. K., Roder, H. (1994) *Biochemistry 33*, 6925−6935.

BI027310+